Thermodynamics and Long-Range Order of Interstitials in an h.c.p. Lattice

Somers, M.A.J.; Kooi, B.J.; Maldzinski, L.; Mittemeijer, E.J.; Kraan, A.M. van der; van der Pers, N.M.

Published in:
Acta Materialia

DOI:
10.1016/S1359-6454(96)00307-2

Publication date:
1997

Pergamon

PII: S1359-6454(96)00307-2

Acta mater. Vol. 45, No. 5, pp. 2013–2025, 1997

1359-6454/97 $17.00 + 0.00

THERMODYNAMICS AND LONG-RANGE ORDER OF INTERSTITIALS IN AN h.c.p. LATTICE: NITROGEN IN ε-Fe_2N_{1-z}

M. A. J. SOMERS[1], B. J. KOOI[1]†, L. MALDZINSKI[2], E. J. MITTEMEIJER[1], A. A. VAN DER HORST[3], A. M. VAN DER KRAAN[3] and N. M. VAN DER PERS[1]

[1]Laboratory of Materials Science, Delft University of Technology, Rotterdamseweg 137, NL-2628 AL Delft, The Netherlands, [2]Instytut Technologii Budowy Maszyn, Poznan University of Technology, Poznan, Poland and [3]Interfaculty Reactor Institute, Delft University of Technology, Mekelweg 15, NL-2629 JB Delft, The Netherlands

(Received 18 June 1995; accepted 2 August 1996)

Abstract—The thermodynamics of nitrogen in the ε-Fe_2N_{1-z} phase were evaluated. To this end absorption isotherms for nitrogen in ε-Fe_2N_{1-z}, depicting the dependence of the nitrogen content on the applied chemical potential of nitrogen, were determined in the temperature range 673–823 K by equilibrating iron foils in gaseous ammonia/hydrogen mixtures. The absorption isotherms could be described very well by a Gorsky–Bragg–Williams approximation for long-range order (LRO) of nitrogen atoms on the hexagonal nitrogen sublattice, formed by the octahedral interstices of the h.c.p. sublattice of iron atoms. The actual occurrence of LRO was evidenced by diffraction analysis. Mössbauer spectra were interpreted as composed of spectra of iron atoms surrounded by 1–3 nitrogen atoms. The relative amounts of the iron environments as determined from the Mössbauer spectra agreed very well with the corresponding probabilities predicted by the LRO model. © *1997 Acta Metallurgica Inc.*

1. INTRODUCTION

The thermodynamics of Fe–N phases and the associated Fe–N phase diagram are of crucial importance in understanding material behaviour observed in the practice of nitriding of iron and steels. The Fe–N phases of major importance are the nitrides γ'-Fe_4N_{1-x} and ε-Fe_2N_{1-z}. Both nitrides can be conceived of as a close-packed sublattice of iron atoms (f.c.c. for γ' [1] and h.c.p. for ε [2]), where nitrogen atoms reside in an ordered way on (a part of) the N-sublattice formed by the octahedral interstices of the Fe-sublattice [1, 2].

For a thermodynamic description of the ε-phase and the γ'-phase, it has been proposed that the Hillert–Staffanson approach [3–12] would apply, i.e. thermodynamically these phases could be regarded as a (sub)regular solution of stoichiometric groups Fe_uN_v and Fe_uV_v (with V vacancies on the N-sublattice) [5–12], where u and v refer to the numbers of sites considered for occupation on the Fe- and N-sublattices, respectively. It was shown recently that this approach does not provide an accurate description of the experimental data (nitrogen-absorption isotherms) for the γ'-phase [13]. This is also expected to be the case for the ε-phase. Therefore, more elaborate models appear in order.

Recently, a model was developed that describes thermodynamics and long-range order (LRO) of interstitials in the octahedral interstices of an h.c.p. host lattice of metal atoms [14]. This model makes use of the Gorsky–Bragg–Williams approximation (or zeroth approximation to long-range ordered solutions) [15, 16], starting with a simple hexagonal sublattice for occupation by interstitials. The model allows the derivation of the ground-state structures (at $T = 0$ K) for this type of interpenetrating h.c.p. and hexagonal sublattice. It provided the corresponding Gibbs free energy and the occupation of the sites of the interstitial sublattice at $T > 0$ K [14]. Among the ground-state structures obtained were the two reported to have been observed experimentally for ε-Fe_2N_{1-z} [2].

In the present paper experimental data on the thermodynamics and the occupancies of the interstitial sites by nitrogen atoms in ε-Fe_2N_{1-z} are presented and the applicability of the model is verified. The thermodynamics are evaluated from experimentally determined nitrogen-absorption isotherms, depicting the relationship between the equilibrium nitrogen content (in the ε-phase) and the nitrogen activity as imposed by a gas mixture, at various gas compositions and temperatures. The occurrence of LRO and the occupancies of the sites of the sublattice of interstitials with nitrogen atoms are investigated applying diffraction analysis and Mössbauer spectroscopy.

†Now at: Dept Applied Physics, Materials Science Centre, University of Groningen, Nijenborgh 4, NL-9747 AG Groningen, The Netherlands.

2. LONG-RANGE ORDER OF NITROGEN IN ε-Fe_2N_{1-z}

2.1. LRO-model

A synopsis of the LRO model for interstitials in the octahedral interstices of an h.c.p. lattice as derived in Ref. 14 is given here. The model assumes a full occupancy of the h.c.p. host lattice with metal atoms (M) and a variable, fractional occupancy of the hexagonal interstitial sublattice with interstitial atoms (I), complemented with vacancies ("atoms" V). Six kinds of sites (A1, B1, ..., C2) are distinguished on this sublattice (Fig. 1). As a consequence of the crystallographic anisotropy of the hexagonal sublattice, pairwise interactions of I atoms within planes parallel to the basal plane [referred to as the (001) plane hereafter] and pairwise interactions in a direction perpendicular to the (001) plane are characterized by different exchange energies per atom, W_p and W_c, respectively (see Fig. 1; cf. Ref. 14):

$$W_p = 3\,[2\,e_{p,\mathrm{IV}} - e_{p,\mathrm{II}} - e_{p,\mathrm{VV}}] \tag{1a}$$

$$W_c = [2\,e_{c,\mathrm{IV}} - e_{c,\mathrm{II}} - e_{c,\mathrm{VV}}] \tag{1b}$$

where $e_{i,JK}$ is the interaction energy of atoms J and K in the direction denoted by i (p = parallel to the basal plane, c = perpendicular to the basal plane). Then, applying the Gorsky–Bragg–Williams approximation [15, 16], the Gibbs free energy of an M–I assembly containing 6N sites on the h.c.p. sublattice (all occupied by M) and N sites for *each* of the six kinds of site of the hexagonal sublattice containing I and V is given by [14]

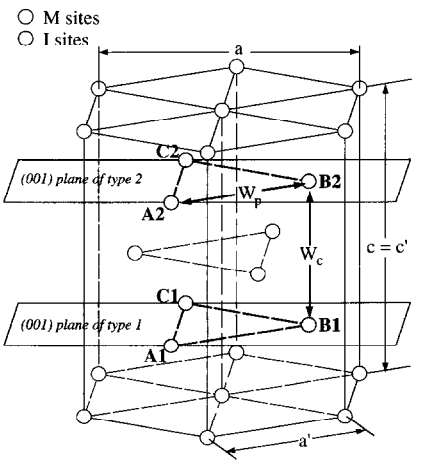

Fig. 1. Three unit cells of the h.c.p. sublattice of M atoms containing one unit cell of the hexagonal sublattice of I atoms. The I sublattice is composed of planes of type 1 and type 2, together having six kinds of site (denoted by A1, B1, C1, A2, B2 and C2) which constitute a trigonal prism. Exchange energies W_p and W_c are operative in the directions indicated. The lattice parameters a and c, a' and c' are indicated [cf. Section 3.2 and equation (8)].

$$\begin{aligned} G_{\mathrm{M-I}} = 6(H^0_{\mathrm{M}} - TS^0_{\mathrm{vib,M}}) + \sum_{K=\mathrm{A1}}^{\mathrm{C2}} [{}^{K}y][H^0_{\mathrm{I}} - TS^0_{\mathrm{vib,I}} \\ + H^0_{\mathrm{MI}} + NW_c + NW_p] - 2NW_c[{}^{\mathrm{A1}}y^{\mathrm{A2}}y + {}^{\mathrm{B1}}y^{\mathrm{B2}}y \\ + {}^{\mathrm{C1}}y^{\mathrm{C2}}y] - NW_p[{}^{\mathrm{A1}}y^{\mathrm{B1}}y + {}^{\mathrm{A1}}y^{\mathrm{C1}}y + {}^{\mathrm{B1}}y^{\mathrm{C1}}y \\ + {}^{\mathrm{A2}}y^{\mathrm{B2}}y + {}^{\mathrm{A2}}y^{\mathrm{C2}}y + {}^{\mathrm{B2}}y^{\mathrm{C2}}y] \\ + NkT \sum_{K=\mathrm{A1}}^{\mathrm{C2}} [{}^{K}y\ln {}^{K}y + (1 - {}^{K}y)\ln(1 - {}^{K}y)] \end{aligned} \tag{2}$$

where T is the temperature, H^0_Q is the enthalpy of N atoms of the pure component Q (with the same lattice as the sublattice considered) and $S^0_{\mathrm{vib,Q}}$ is the vibrational entropy of N atoms of the pure component Q, which is assumed to be independent of composition and ordering. Further, H^0_{MI} is the enthalpy of the interaction of N atoms of M and N atoms of I, k being the Boltzmann constant and ${}^{K}y$ the fraction of sites of kind K that is occupied by atoms I.

The chemical potential for N atoms I at each of the sublattices formed by sites of kind K, ${}^{K}\mu_{\mathrm{I}}$, is, as for an open system (V represents vacancies), by definition given by

$${}^{K}\mu_{\mathrm{I}} = \left(\frac{\partial G_{\mathrm{M\,I}}}{\partial {}^{K}y}\right)_{p,\,T,\,{}^{J}y(\neq {}^{K}y)}. \tag{3}$$

Using equation (2) gives, for K = A1,

$$\begin{aligned} {}^{\mathrm{A1}}\mu_{\mathrm{I}} = \mu^0_{\mathrm{I}} - 2NW_c[{}^{\mathrm{A2}}y] - NW_p[{}^{\mathrm{B1}}y + {}^{\mathrm{C1}}y] \\ + NkT\ln\left[\frac{{}^{\mathrm{A1}}y}{1 - {}^{\mathrm{A1}}y}\right] \end{aligned} \tag{4}$$

where $\mu^0_{\mathrm{I}} = (H^0_{\mathrm{I}} - TS^0_{\mathrm{vib,I}} + H^0_{\mathrm{MI}} + NW_c + NW_p)$. Expressions for ${}^{K}\mu_{\mathrm{I}}$ of the I atoms on the other kinds of sites K are similar to equation (4).

Thermodynamic equilibrium for this M–I solid solution involves equal chemical potentials ${}^{K}\mu_{\mathrm{I}}$ of the interstitial element I on the six kinds of I site, i.e.

$${}^{\mathrm{A1}}\mu_{\mathrm{I}} = {}^{\mathrm{B1}}\mu_{\mathrm{I}} = {}^{\mathrm{C1}}\mu_{\mathrm{I}} = {}^{\mathrm{A2}}\mu_{\mathrm{I}} = {}^{\mathrm{B2}}\mu_{\mathrm{I}} = {}^{\mathrm{C2}}\mu_{\mathrm{I}} \equiv \mu_{\mathrm{I}}. \tag{5}$$

For given values of the interaction energies W_c and W_p, the chemical potential of the interstitial atoms and the evolution of the occupancies of the different kinds of sites can be evaluated from equations (4) and (5). For mutual repulsion of the interstitials, i.e. $W_c < 0$ and $W_p < 0$, two ground-state structures were found for the ordered configuration of atoms I on their sublattice. These were denoted as Configuration A and Configuration B. Configuration A is characterized by an alternation of (001) planes with compositions I_2V and V_2I; for Configuration B these planes have equal compositions.

It was shown in Ref. 14 that for an arbitrary combination of negative values for the interaction energies W_p and W_c, generally Configuration A is the most stable one for compositions close to M_2I, whereas Configuration B is the most stable one for

lower interstitial contents (close to M_3I). The transition from Configuration A to B and vice versa was found to be a first order phase transition, whereas the order–disorder transition itself is a second order phase transition.

2.2. *Experimental verification*

Nitrogen-absorption isotherms depict the dependence of the total nitrogen content in ε-Fe_2N_{1-z}, $y_N = \frac{1}{6}\sum_{J=A1}^{C2} {}^{J}y$, on the chemical potential of nitrogen, μ_N, as imposed by a gas mixture. Combining such experimental absorption isotherms with equations (4) and (5), where M = Fe and I = N, for either Configuration A or Configuration B, yields values for the occupancies of each of the sites A1, . . ., C2 and the interaction energies W_p and W_c.

An equilibrium state of ε-Fe_2N_{1-z} cannot be attained with pure nitrogen gas at atmospheric pressure, because equilibrium partial pressures of nitrogen amount to several GPa for this iron nitride (at normal temperatures: 500–1000 K). Ammonia/hydrogen gas mixtures are suitable for investigating the thermodynamics of Fe–N phases at atmospheric pressure. The chemical potential of nitrogen in an NH_3/H_2 mixture, $\mu_{N,g}$, can be defined on the basis of the hypothetical equilibrium:

$$NH_3 \rightleftarrows \tfrac{1}{2}N_2 + \tfrac{3}{2}H_2 \qquad (6a)$$

where

$$\mu_{N,g} = \tfrac{1}{2}\mu_{N_2} = \mu_{NH_3} - \tfrac{3}{2}\mu_{H_2}. \qquad (6b)$$

If ideal gases or constant fugacity coefficients can be assumed, then

$$\mu_{N,g} = \tfrac{1}{2}G^0_{N_2} + \tfrac{1}{2}RT\ln\frac{p_{N_2}}{p^0}$$

$$= G^0_{NH_3} - \tfrac{3}{2}G^0_{H_2} + \tfrac{1}{2}RT\ln p^0 + RT\ln r_N \qquad (6c)$$

with

$$r_N = \frac{p_{NH_3}}{p_{H_2}^{3/2}}$$

where p_j refers to the partial pressure of j, p^0 is the reference pressure which is taken as unit pressure, the superscript 0 indicates the standard state (with reference to unit pressure) of the component concerned and r_N is the so-called nitriding potential. The virtual partial pressure of N_2 corresponding to an NH_3/H_2 mixture can be calculated from equation (6). Equilibrium between gas atmosphere and solid ε implies $\mu_{N,g} = \mu_{N,s}$ where $\mu_{N,s}$ has to be substituted for ${}^{A1}\mu_I = \mu_I$ in equations (4) and (5). Taking μ_I in equation (4) for one mole of nitrogen atoms, and thus the symbol N in equation (4) equals Avogadro's number, it follows from equating equations (4) and (6) that

$$\ln\frac{r_N}{r_N^0} = \ln\left[\frac{{}^{A1}y}{1-{}^{A1}y}\right] + (1-2\,{}^{A2}y)\frac{W_c}{RT}$$

$$+ (1-{}^{B1}y-{}^{C1}y)\frac{W_p}{RT} \qquad (7)$$

with r_N^0 defined as

$$RT\ln r_N^0 = G_N^0 - G^0_{NH_3} + \tfrac{3}{2}G^0_{H_2}$$

and

$$G_N^0 = H_N^0 - TS^0_{vib,N} + H^0_{FeN}.$$

W_c, W_p, H_N^0, $S^0_{vib,N}$ and H^0_{FeN} now hold per mole of nitrogen atoms. It follows from equation (7) that r_N^0 can be interpreted as the nitriding potential in equilibrium with ε-Fe_2N_{1-z}, having the hypothetical composition Fe_2N and ${}^{A1}y = {}^{B1}y = {}^{C1}y = {}^{A2}y = {}^{B2}y = {}^{C2}y = \frac{1}{2}$ (i.e. a random distribution of N atoms over all available sites). For the other kinds of sites, equations similar to equation (7) hold. Fitting the set of equations (7) to the experimentally determined dependence of

$$y_N = \tfrac{1}{6}\sum_{J=A1}^{C2} {}^{J}y$$

on r_N leads to values for W_c, W_p, ${}^{K}y$ and r_N^0; the values for W_c and W_p determine the values for ${}^{K}y$ [14].

3. EXPERIMENTAL

3.1. *Determination of nitrogen-absorption isotherms*

The manufacturing of *homogeneous* Fe–N phases is difficult. A porous iron foil as a starting material is advantageous for studying the equilibrium of Fe–N phases with a gas mixture of known composition (see Appendix for further discussion).

The present ε-nitrides were produced by nitriding a porous iron foil in ammonia/hydrogen mixtures. Pure iron (chemical composition: 0.03 wt% C, 0.01 wt% Ni, 0.003 wt% Si and traces of Mg, Cu, Ag, Co, Al, Ca and Ge; balance: Fe) was cold-rolled to a thickness of 50 μm and cleaned in acetone. Foils of 500 × 15 × 0.05 mm^3 were supported by a quartz specimen holder. Experimental details of the prenitriding treatments used to make the foils porous have been provided elsewhere [8, 17].

Nitrogen-absorption isotherms were determined thermogravimetrically. Experimental details of the gas purification, as well as the adjustment and control of the gas mixture have been given in Refs 8 and 17. All (stationary) sample weight increases were converted to nitrogen contents, after correction for buoyancy effects.

Nitrided porous foils, used for diffraction analysis and Mössbauer spectroscopy, were produced at selected temperatures and nitriding potentials such that the compositions covered the range from $Fe_2N_{2/3}$ to Fe_2N_1. After nitriding, these samples were either

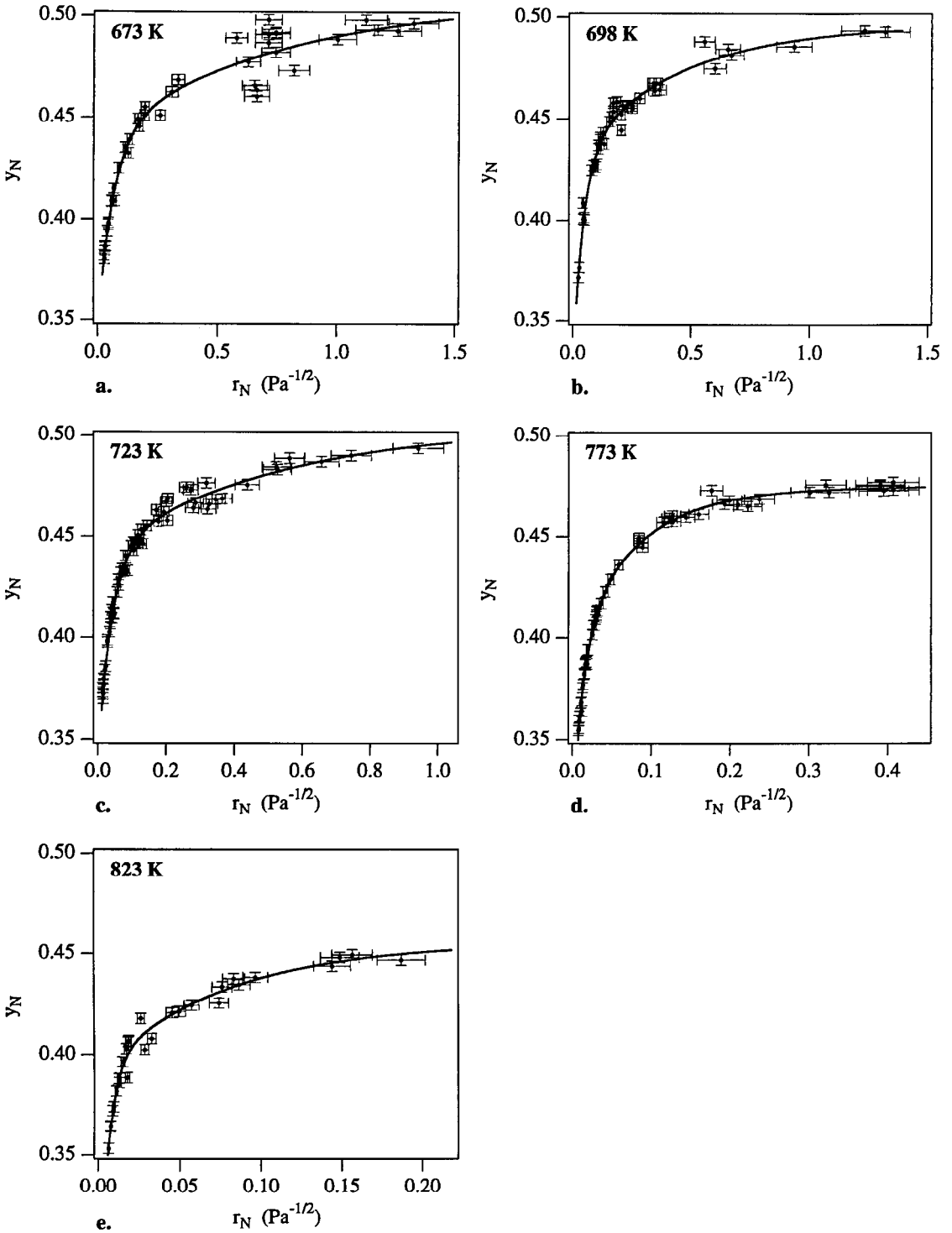

Fig. 2. Nitrogen absorption isotherms for ε-Fe_2N_{1-z} ($y_N = \frac{1}{2}(1 - z)$) at (a) 673 K, (b) 698 K, (c) 723 K, (d) 773 K and (e) 823 K. Lines were obtained by fitting a double exponential function and are meant to guide the eye.

cooled moderately fast or quenched after a constant mass of the specimen was attained upon nitriding. For reference an ε-Fe_2N_{1-z} powder of composition $Fe_2N_{2/3}$ was used [22].

3.2. X-ray and neutron diffraction analysis

Parts of nitrided porous foils were powdered and investigated with X-ray diffraction analysis (XRD) to

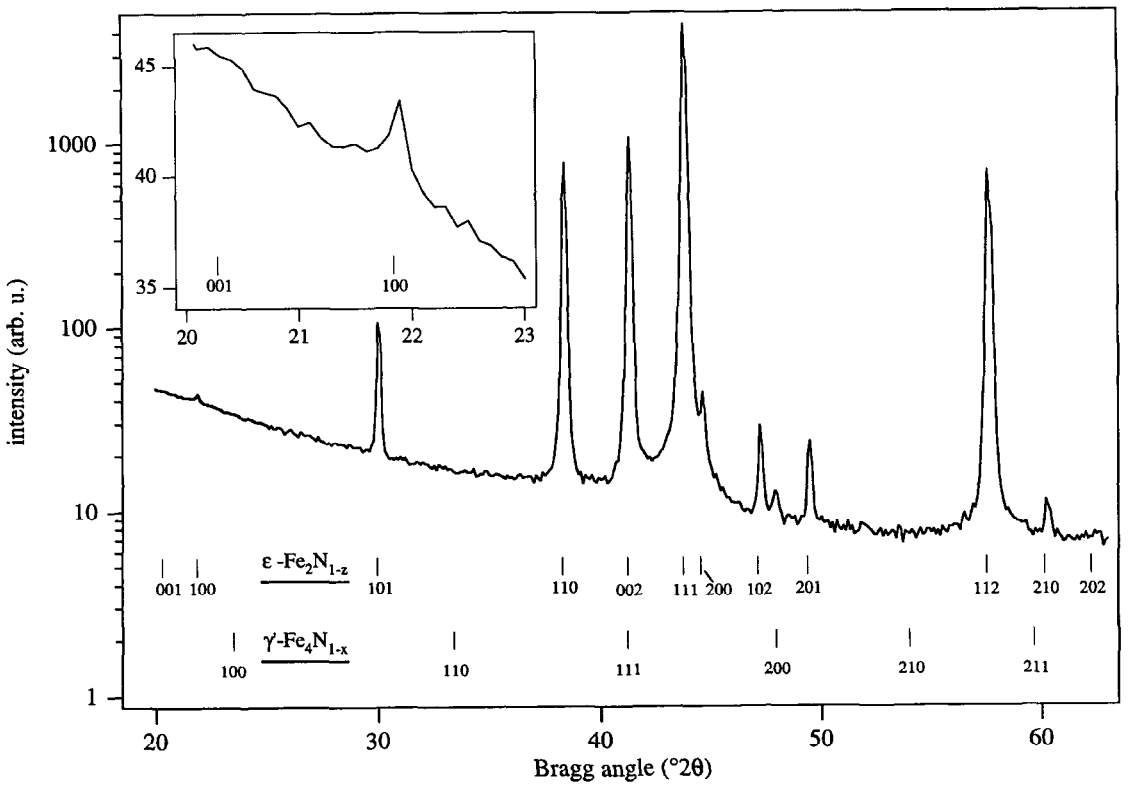

Fig. 3. X-ray diffractogram of reference powder ε-$Fe_2N_{2/3}$. The 2θ positions of the reflections pertaining to γ'-Fe_4N_{1-x} and ε-Fe_2N_{1-z} and the corresponding Laue indices of the reflections have been indicated.

determine the a and c lattice parameters of the hexagonal ε-phase and to determine the ground-state structure (type of order). XRD was performed on a Siemens D-500 goniometer with $CuK_{\alpha_{1,2}}$ or $CoK_{\alpha_{1,2}}$ radiation. Survey scans within the range of 15–165° for 2θ were recorded for phase identification. For the determination of the a and c lattice parameters accurate scans were made of the {110}, {111} and {112} line profiles.† The two lattice parameters a and c were determined from the 2θ peak positions of these ($11l$) reflections (cf. Ref. 18). The reference powder was similarly investigated. Some of the samples were investigated with neutron diffraction at the High Flux Reactor of the Netherlands Energy Research Centre (ECN in Petten, The Netherlands).

3.3. *Mössbauer spectroscopy*

The samples investigated consisted of a mosaic of small flakes broken from the brittle nitrided porous foils. The reference powder sample was investigated as it was.

Mössbauer spectra were recorded with a constant acceleration spectrometer using a ^{57}Co in Rh source. Isomer shifts were recorded with respect to the NBS standard sodium nitroprusside. The spectrometer was calibrated by the 515 kOe hyperfine field of α-Fe_2O_3 at room temperature.

The Curie temperature of ε-Fe_2N_{1-z} varies from about 560 K for $Fe_2N_{2/3}$ to <4.2 K for a composition close to Fe_2N [19]. Therefore, Mössbauer spectroscopy was carried out at 4.2 K (boiling He). Cooling did not modify the Mössbauer spectra.

The Mössbauer spectra were interpreted as composed of a combination of sextuplets for the iron atoms surrounded by a specific number of nitrogen neighbours (in principle from 0 up to 6). Details about the procedure for the evaluation of the hyperfine parameters and the abundances of the various iron environments are given in Ref. 17.

4. RESULTS

4.1. *Nitrogen-absorption isotherms*

The nitrogen-absorption isotherms as determined for ε-Fe_2N_{1-z} at 623 K, 673 K, 723 K, 773 K and 823 K are shown in Fig. 2. According to the isotherms at 673 K, 698 K and 723 K the maximum nitrogen content for the ε-phase appears to be $y_N = 0.5$ (50 at.N/100 at.Fe; $z = 0$). At 773 K and 823 K the maximum nitrogen content dissolved is clearly less than 50 at.N/100 at.Fe, which is attributed to the occurrence of a stationary state at the

†In the present paper, {hkl} refers to the Miller indices of the unit cell accounting for the two types of ordering of the nitrogen atoms as proposed in Ref. 2. As compared to the h.c.p. iron sublattice, having lattice parameters a' and c', this unit cell has lattice parameters $a = a'\sqrt{3}$ and $c = c'$ [2] (see Fig. 1).

interface of the solid sample and the gas mixture. This stationary state results from the competition between the dissolution of nitrogen atoms adsorbed at the surface into the ε-phase and the association of adsorbed nitrogen atoms to molecular nitrogen at the surface and its subsequent desorption (see Appendix). Consequently, the experimental nitrogen-absorption isotherms at 773 K and 823 K cannot be used for testing the model for nitrogen ordering that leads to the set of equations (7).

4.2. X-ray and neutron diffraction analysis

The X-ray diffractogram of the reference ε-nitride powder is given in Fig. 3. The occurrence of LRO of the nitrogen atoms on their own sublattice follows from the occurrence of lines in the diffractogram of the ε-phase that are forbidden for an h.c.p. lattice of pure iron; these lines are referred to as "superstructure" reflections (relative to the h.c.p. lattice of the iron atoms). Evidence for the occurrence of ordering of the nitrogen atoms was obtained for all samples by the presence of the {101} "superstructure" reflections (cf. Fig. 3). The type of LRO can be deduced from comparison of the measured intensity values of the "superstructure" reflections with calculated intensity values for a specific type of order: the presence of {001} corresponds to the occurrence of Configuration A; the presence of {100} (and of {102}) corresponds to the occurrence of Configuration B.

Conclusive diffraction evidence regarding the type of order was only obtained for the very slowly cooled reference ε powder [22] of composition $Fe_2N_{2/3}$, where the {100} reflection appears and thus the nitrogen atoms are ordered according to Configuration B (see Fig. 3). Rietveld refinement of the corresponding neutron diffraction pattern indicated almost full occupancy of sites A1 and B2 (cf. Fig. 1) with N atoms [18], implying almost perfect ordering of the nitrogen atoms according to Configuration B.

No conclusive evidence was obtained for the occurrence of Configuration A or Configuration B in the powdered nitrided foils: neither X-ray nor neutron diffractograms showed {100} and {001} "superreflections". Thus it is concluded that the order parameter for the nitrogen atoms in moderately fast cooled specimens is considerably smaller than 1 or, alternatively, that the ordered domains are very small, leading to broad superstructure reflections of small height.

The measured lattice parameters a and c of the nitrogen sublattice have been given in Fig. 4. Foils prepared near the limits of the composition range for ε and cooled moderately fast to room temperature were not monophase, owing to decomposition during cooling. Foils with compositions corresponding to about $Fe_2N_{2/3}$ ($y_N = \frac{1}{3}$) and to about Fe_2N_1 ($y_N = \frac{1}{2}$) contained γ'-Fe_4N_{1-x} and ζ-Fe_2N, respectively, after cooling. Literature values for the lattice parameters a and c of ε-Fe_2N_{1-z} [20–22] are also shown in Fig. 4, as well as the results from the evaluation given in Ref. 23. Clearly, the more recent and the present lattice-parameter data are well above those evaluated in Ref. 23. The deviation is attributed to the

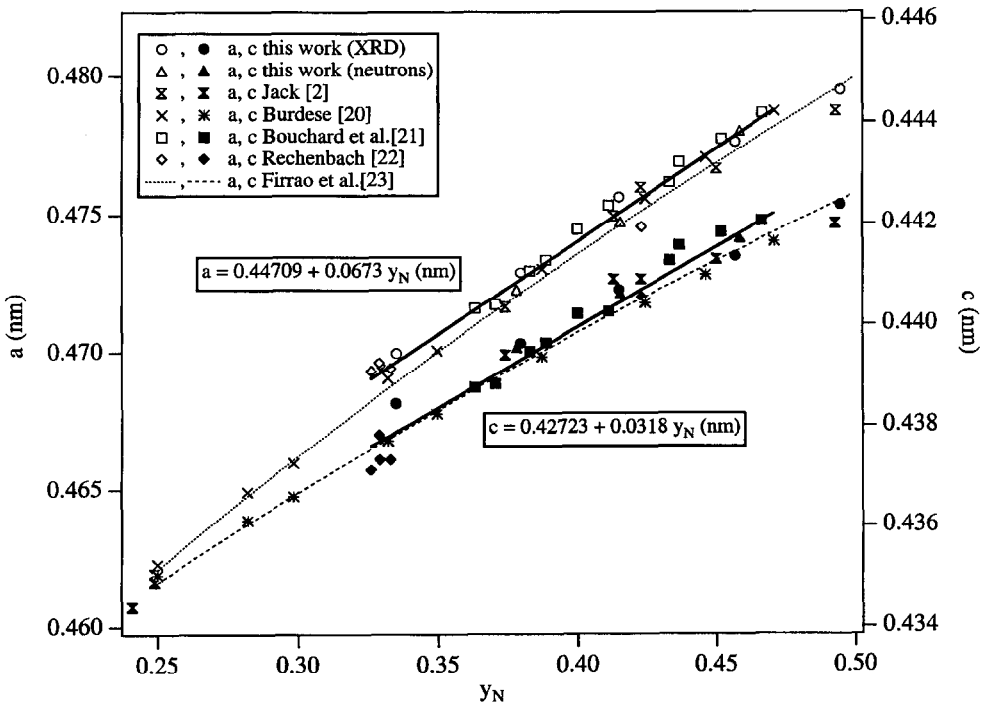

Fig. 4. Dependence of lattice parameters a and c of ε-Fe_2N_{1-z} on the occupancy of the nitrogen sublattice, y_N [$=\frac{1}{2}(1-z)$]. Full lines are fits to the data in the composition range $0.33 \leq y_N \leq 0.47$.

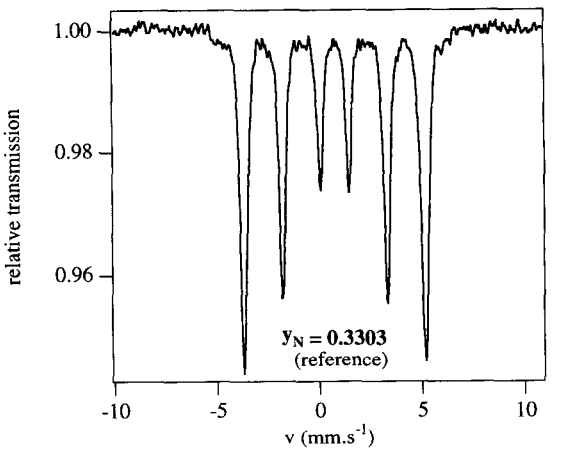

a.

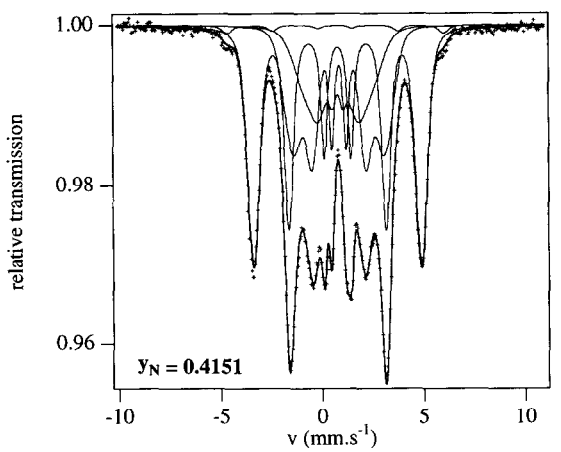

b.

Fig. 5(a). Mössbauer spectrum of ε reference powder (v = Doppler velocity). The specimen is composed predominantly of one sextuplet corresponding to iron atoms surrounded by two nitrogen atoms, which is indicative of Configuration B (see Fig. 1). (b) Mössbauer spectra (data points) recorded for ε-Fe_2N_{1-z} foil with $y_N = 0.4151$. The overall spectrum (bold line) results from summation of the four sextuplets (thin lines).

incorporation of the lattice parameters for ε-$Fe_2(N,C)_{1-z}$, containing carbon, in the evaluation of Ref. 23. A linear dependence of a and c on y_N was assumed for the composition range $y_N = 0.33$ to $y_N = 0.47$ (full straight lines in Fig. 4). The following were obtained:†

$$a = 0.44709 + 0.0673\, y_N \text{ (nm)} \quad (8a)$$

$$c = 0.42723 + 0.0318\, y_N \text{ (nm)} \quad (8b)$$

†The data close to the composition Fe_2N_1 were not incorporated in the evaluation, because they may be affected by the development of ζ-Fe_2N due to decomposition during cooling after nitriding.

where y_N denotes the total fractional occupancy of the interstitial sublattice (=at.N/at.Fe) of ε-Fe_2N_{1-z} [$y_N = \frac{1}{2}(1 - z)$].

4.3. Mössbauer spectroscopical analysis

The Mössbauer spectra measured at $T = 4.2$ K for the ε reference powder ($y_N = 0.3303$) and for one of the ε-Fe_2N_{1-z} foils ($y_N = 0.4151$) are given in Fig. 5. The hyperfine parameters and the relative contribution of the different sextuplets in the enveloping spectrum are given in Table 1 for the reference powder and each of the ε-foils.

The almost perfect order of the nitrogen atoms according to Configuration B in the reference powder is clearly exhibited by its Mössbauer spectrum [Fig. 5(a)]. It is dominated by one sextuplet, which can be attributed to iron atoms surrounded by two nitrogen atoms (denoted as II^e in Table 1). This is the only iron environment occurring for the ground state structure of Configuration B. Also X-ray diffraction data indicated Configuration B for the ε reference powder (see Section 4.2). A small fraction of the iron atoms in the reference powder is surrounded by one nitrogen atom (denoted as I^e), consistent with the slight understoichiometry of the reference powder with respect to $Fe_2N_{2/3}$ ($y_N = 0.3303$ instead of 1/3). The fraction of I^e was not quantified.

A very good description of the experimental Mössbauer spectra recorded from the ε-foils could be obtained by fitting three or four sextuplets [see Fig. 5(b) as a representative example]. For iron atoms surrounded by three nitrogen atoms two sextuplets were identified, which are denoted as III^e(a) and III^e(b) in Table 1. Details of attributing the sextuplets to a particular environment of iron are given in Ref. 17. The total nitrogen content of the samples as calculated from the relative contributions of the various environments is in very good agreement with the nitrogen content determined by thermogravimetry (see Table 1).

5. DISCUSSION

5.1. Nitrogen-absorption isotherms described by the LRO model

A sensitive graphic presentation for comparison of the experimental absorption-isotherm data with the model description of the set of equations (7) is provided by Fig. 6. Here, the nitrogen-absorption isotherm data are given relative to a model that would apply if the nitrogen atoms were distributed randomly over only half of the total amount of the sites of the interstitial sublattice (a Langmuir-type approach for $Fe_2(N, V)$; cf. the consideration for γ'-Fe_4N_{1-x} in Ref. 13). The parameter given at the ordinate in Fig. 6 and studied as a function of y_N obeys

$$f(y_N) = \ln r_N - \ln\left[\frac{2\, y_N}{1 - 2\, y_N}\right].$$

Table 1. Hyperfine field (H), isomer shift (δ) and relative contribution (f) of sextuplets designated by I^ε, II^ε, III^ε (a) and III^ε (b) to Mössbauer spectra of ε-Fe_2N_{1-z} reference powder ($y_N = 0.3303$), and ε-Fe_2N_{1-z} foils Σf_i (%) $= y_N$ is the total fraction of interstitial sites occupied by nitrogen atoms as calculated from the relative contributions of iron atoms surrounded by $i = 0, 1 \ldots 6$ nitrogen atoms (there is one N site per Fe atom and each Fe atom is surrounded by six different sites)

	I^ε			II^ε			III^ε (a)			III^ε (b)			
y_N	H (kOe)	δ (mm/s)	f	H (kOe)	δ (mm/s)	f	H (kOe)	δ (mm/s)	f	H (kOe)	δ (mm/s)	f	Σf_i(%)
0.3303	—	—	~0	271.8	0.72	~1	—	—	~0	—	—	~0	0.3333
0.3351	330.3	0.64	0.12	256.6	0.73	0.68	147.3	0.79	0.201	—	—	~0	0.3472
0.3795	334.0†	0.66	0.072	256.7	0.74	0.578	147.3	0.82	0.221	110.2	0.75	0.129	0.3797
0.4151	334.0†	0.66	0.01	258.8	0.75	0.454	140.7	0.82	0.327	97.4	0.76	0.204	0.4185
0.4568	—	—	—	254.6	0.76	0.262	138.5	0.82	0.308	86.0†	0.79	0.430	0.4563

†Fixed value in the fitting procedure; chosen by trial and error.

It is demonstrated in Ref. 17 that the zeroth approximation to a regular solution [cf. 5, 6], the subregular solution model [cf. 7–9], a Wagner–Schottky approach for $y_N = 0.5$ [cf. 13] and a Gorky–Bragg–Williams approximation with site exclusion [24] cannot adequately describe the experimental absorption isotherms.

The nitrogen-absorption isotherms determined at 673 K, 698 K and 723 K were used for testing the validity of the model [equation (7)], because they represent equilibrium of the sample composition with the imposed gas atmosphere (see Section 4.1). In order to investigate the consistency of the set of equations (7) with the nitrogen-absorption isotherms, these equations were fitted simultaneously to the three absorption isotherms for a chosen configuration (either A or B) and an assumed temperature dependence for the interaction energies W_p and W_c. It was assumed that the exchange energies W_j either obeyed $W_j =$ constant or $W_j/T =$ constant.† The value for $\ln r_N^0$ [see below equation (7)] was taken as $p/T + q$, with p and q as fitting parameters. On this basis only four fitting parameters were assessed in the fitting of the set of equation (7) to the three absorption isotherms: W_p, W_c, p and q (for more details about the fitting procedure, see Ref. 17). The values thus obtained for W_p, W_c and $\ln r_N^0$ for the four possible combinations of two order configurations and two temperature dependencies for the exchange energies, are given in Table 2.

Qualitatively, taking repulsion between nitrogen atoms for granted, it is expected that the value for the exchange energy per bond in the direction perpendicular to the basal plane (c-direction) of the hexagonal unit cell, W_c, is more negative than the value for the exchange energy per bond within the basal plane, $W_p/3$ [see equation (1)], because neighbouring sites in the c-direction are nearer than those in the basal plane. The ratios $W_c/\frac{1}{3}W_p$ for the four combinations considered in Table 2 are given in Table 3a. Indeed, for the four cases considered $|W_c| > \frac{1}{3}|W_p|$. If the mutual repulsion of the nitrogen atoms were due to electronic (chemical bonding) effects, the interaction energy of two similarly charged nitrogen atoms is anticipated to depend inversely on the separation distance of the nitrogen atoms. If strain effects, due to misfitting of nitrogen atoms in the octahedral interstices, were responsible for mutual repulsion, this interaction energy is anticipated to depend reciprocally on the cube of the separation distance of the nitrogen atoms [25, 26]. The separation distances between neighbouring interstitial sites in the basal plane, r_p, and in the c direction, r_c, were obtained using equation (8) ($r_p = a/\sqrt{3}$ and $r_c = c/2$). Values for (r_p/r_c) and $(r_p/r_c)^3$ are given in Table 3b.

Assuming, $W_c/\frac{1}{3}W_p = (r_p/r_c)^n$ (with $n = 1$ or 3), the values in Tables 3a and 3b indicate that the results obtained for Configuration B (Table 2) do not agree at all with the $(r_p/r_c)^n$ ratios, whereas such agreement exists for Configuration A. If the proposed LRO model applies, a single set of W_c, W_p and $\ln r_N^0$ values should hold for both Configuration A and Configuration B. Configuration A prevails at least for nitrogen contents higher than about $y_N = 0.4$ (see Section 5.3 and Ref. 14). Consequently, recognizing that W_c controls the absorption isotherm at high values of y_N [17], the value for W_c for Configuration A is likely to be correct. The value obtained for Configuration A for $W_c/\frac{1}{3}W_p$ with $W_j/T =$ constant is very close to the value expected for the interaction of nitrogen atoms due to elastic strains (cf. Tables 3a and 3b). Accordingly, it is concluded that, within the composition range and (relatively small) temperature range investigated, Configuration A can be adopted to describe the absorption isotherms, taking W_j as directly proportional to temperature.

5.2. *Site occupancies for the nitrogen sublattice*

Values for the occupancies, ${}^K y$ ($K =$ A1, . . ., C2) of sites A1, . . ., C2 (Fig. 1) are obtained on fitting the set of equations (7) to the absorption-isotherm data. The dependencies of the occupancies of the six kinds of sites for nitrogen atoms on the total occupancy of the interstitial sublattice are similar to those given in Figs 5 and 6 of Ref. 14. From the occupancies, ${}^K y$, the probabilities, p_i ($i = 0, \ldots, 6$), for iron atoms

†An immediate consequence of assuming $W_j/T =$ constant is that the stability ranges of the Configurations A and B do not depend on the temperature and that no critical temperature for disordering exists (cf. Fig. 8 in Ref. 14). This is unrealistic, but the assumption may be justified for a relatively small temperature range as in the present case.

surrounded by 0–6 nitrogen atoms were calculated straightforwardly, and are shown for iron atoms surrounded by 1–4 nitrogen atoms in Fig. 7 (the probabilities for iron atoms surrounded by 0, 5 and 6 nitrogen atoms are negligibly small). In Fig. 7, the probabilities calculated with the values in Table 2 for

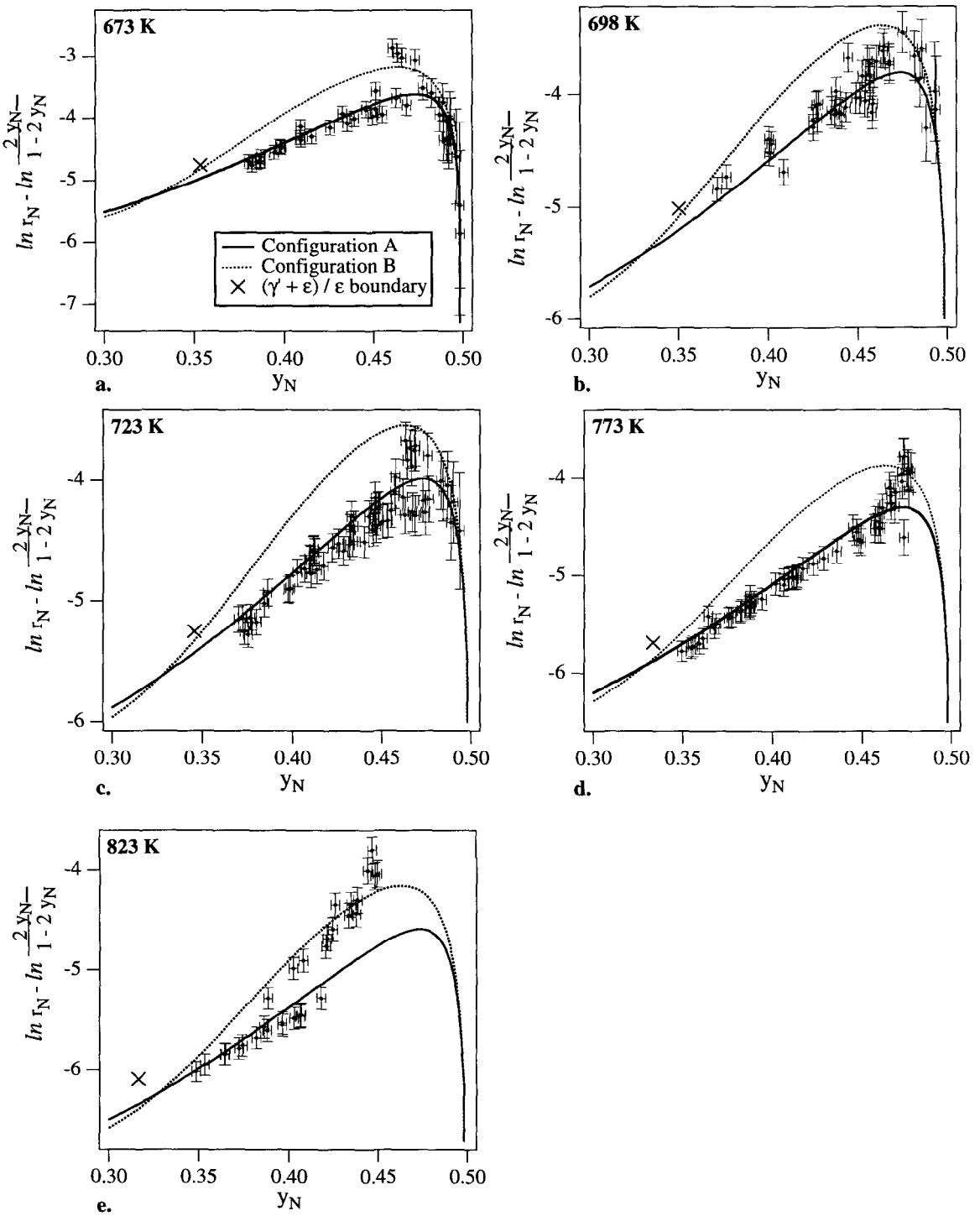

Fig. 6. Experimental nitrogen-absorption isotherms (data points) for ε-Fe_2N_{1-z} [$y_N = \frac{1}{2}(1-z)$] at (a) 673 K, (b) 698 K, (c) 723 K, (d) 773 K and (e) 823 K; r_N in $Pa^{-1/2}$. The lines drawn indicate the absorption isotherms for both Configuration A and B as described by the set of equations (7) using values for W_c, W_p and $\ln r_N^0$ as obtained by fitting Configuration A to the experimental data at 673 K, 698 K and 723 K simultaneously (with W_i/T = constant). Crosses indicate the position of the $\gamma' + \varepsilon/\varepsilon$-phase boundary.

Table 2. Values for W_p, W_c and $\ln r_N^0$ obtained on fitting the set of equations (7) simultaneously to the absorption isotherm data at 673 K, 698 K and 723 K, assuming W_j = constant or W_j/T = constant (j = p,c) for Configuration A and Configuration B

	W_j = constant			W_j/T = constant		
	W_p/R (K)	W_c/R (K)	$\ln r_N^0$ (r_N^0 in $Pa^{-1/2}$)	W_p/RT	W_c/RT	$\ln r_N^0$ (r_N^0 in $Pa^{-1/2}$)
Configuration A	−3682	−1840	$6110/T - 8.634$	−4.48	−2.98	$3591/T - 4.923$
Configuration B	−1257	−3307	$5850/T - 8.274$	−1.21	−5.09	$4179/T - 5.833$

Configurations A and B with W_j/T = constant are denoted as p_i A(A) and p_i B(B), respectively; the probabilities calculated for Configuration B with the values in Table 2 for Configuration A with W_j/T = constant are denoted as p_i B(A). The relative abundances, f_i, of iron atoms surrounded by 1–3 nitrogen atoms to Mössbauer spectra (Table 1) are also shown in Fig. 7 [where f_i for III^e(a) and III^e(b) have been summed and are denoted as f_3 for III^e].

Very good agreement is observed between calculated probabilities p_2 and p_3 and measured relative abundances f_2 and f_3 at $y_N = 0.3351$ for Configuration B [p_2 B(A) and p_3 B(A)] and at $y_N = 0.4568$ for Configuration A. [Note that iron surrounded by two and three nitrogen atoms dominates the Mössbauer spectrum (see Table 1c).] This result agrees with the expectation that Configuration B is favoured for compositions close to $Fe_2N_{2/3}$ and Configuration A is favoured for compositions close to Fe_2N_1 (see Refs 2 and 14). For intermediate nitrogen contents ($y_N = 0.3795$ and $y_N = 0.4151$) the measured relative abundances of II^e and III^e are in between the calculated probabilities for Configuration A and Configuration B (with W_p/T and W_c/T as for Configuration A). This experimental result strongly suggests the occurrence of a two-phase region for ε-Fe_2N_{1-z} where a phase of Configuration A is in equilibrium with a phase of Configuration B. A two-phase region of Configurations A and B was also predicted from model calculations for the present LRO model (see Fig. 8 of Ref. 14).

The relative abundance of I^e seems to follow the probability, p_1, calculated for Configuration B (with W_p/T and W_c/T as for Configuration A). This result is attributed to the relatively poor quantification of this small contribution to the Mössbauer spectra. For the same reason, the small contribution of iron atoms surrounded by four nitrogen atoms, which would appear as a single peak in the Mössbauer spectra, remained unobserved.

The probabilities p_i B(B) do not agree with the measured values for the relative abundances f_i. This is illustrated in particular at low nitrogen contents for iron atoms surrounded by two nitrogen atoms (II^e in Fig. 7). This demonstrates that the W_j values for Configuration B in Table 2 are unrealistic (see last paragraph in Section 5.1).

Table 3a. Ratio $W_c/\frac{1}{3}W_p$ for the four possible combinations of two configurations and two assumed temperature dependencies for W_j (cf. Table 2)

	$W_c/\frac{1}{3}W_p$	
	W_j = constant	W_j/T = constant
Configuration A	1.50	2.00
Configuration B	7.89	12.6

Table 3b. Ratios (r_p/r_c) and $(r_p/r_c)^3$ for three nitrogen contents y_N within the composition range of ε-Fe_2N_{1-z} as calculated from the lattice parameters given by equation (8)

y_N	(r_p/r_c)	$(r_p/r_c)^3$
0.33	1.24	1.90
0.40	1.24	1.93
0.47	1.25	1.95

5.3. *Thermodynamics of* ε-Fe_2N_{1-z}

The nitrogen-absorption isotherms for both Configuration A and Configuration B as calculated with the values for W_c, W_p and $\ln r_N^0$ for Configuration A with W_j/T = constant (Table 2) are shown in Fig. 6 together with the experimental data.

The data points corresponding to the $(\gamma' + \varepsilon)/\varepsilon$-phase boundary have also been indicated in Fig. 6 (see crosses). The nitriding potential at the phase boundary pertaining to coexistence of γ'-Fe_4N_{1-x} and ε-Fe_2N_{1-z}, was obtained from the so-called Lehrer diagram; the composition corresponding to the $(\gamma' + \varepsilon)/\varepsilon$-phase boundary was obtained from the Fe–N phase diagram [13]. Comparison of the calculated absorption isotherms for Configuration B, which applies for the low nitrogen contents, to these (independent) data points shows a very good correspondence for the temperatures considered for fitting of the LRO model [Figs 6(a)–(c)]. This result indicates consistency of the LRO model adopted for the ε-phase, using the values for W_c, W_p and $\ln r_N^0$ as obtained by fitting Configuration A to the nitrogen-absorption isotherms.

The absorption isotherms calculated for 773 K and 823 K using the W_c, W_p and $\ln r_N^0$ values determined from the absorption isotherms at 673, 698 and 723 K are shown in Figs 6(d) and (e). Clearly, the calculated absorption isotherms for Configuration B at 773 K and 823 K deviate from the data points pertaining to the $(\gamma' + \varepsilon)/\varepsilon$-phase boundary. This may be related to the temperature dependence adopted for the exchange energies (W_j/T = constant). Adopting W_j = constant leads to a deviation of opposite sign. Further, recognizing that the experimental absorption-isotherm data for $T > 723$ K are affected by the

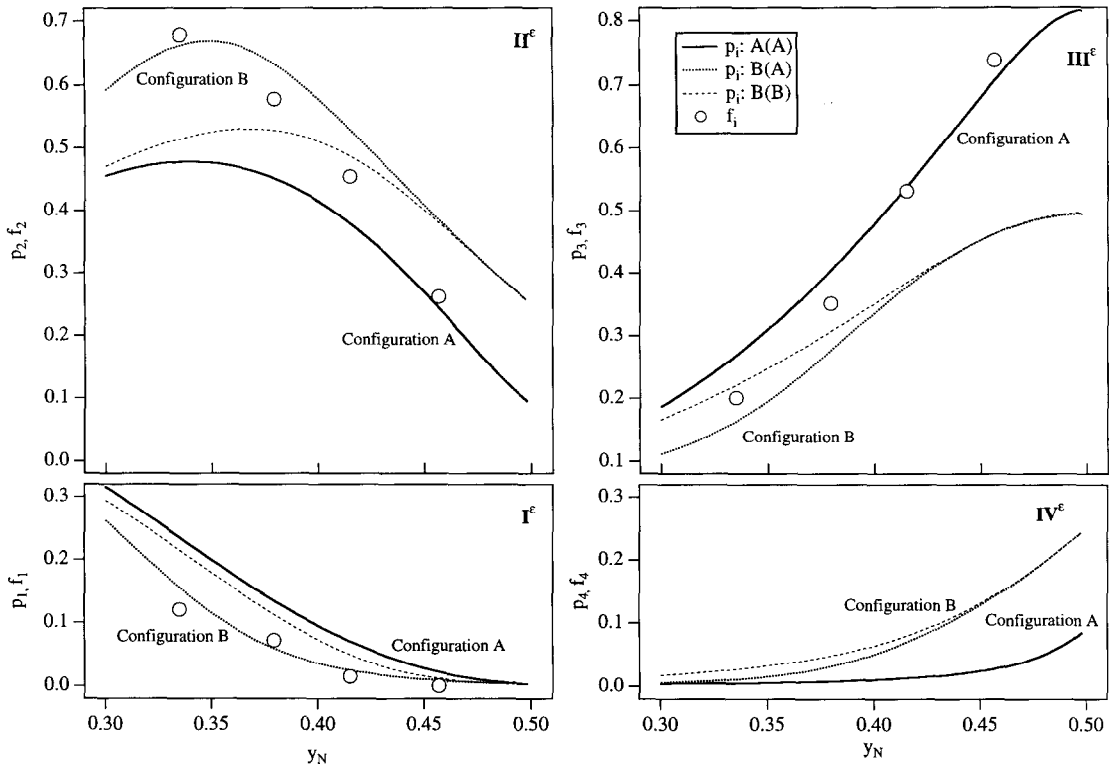

Fig. 7. Relative abundances, f_i, of iron atoms surrounded by 1–3 nitrogen atoms (indicated by I^ε, II^ε, III^ε) as a function of the overall occupancy of the nitrogen sublattice, y_N, shown by dots (Table 1: $III^\varepsilon = III^\varepsilon(a) + III^\varepsilon(b)$). The probabilities, p_i, for iron atoms surrounded by 1–4 nitrogen atoms, as calculated from the individual occupancies of sites A1–C2 (cf. Fig. 1) according to the LRO-model are shown by drawn lines for Configurations A and B for W_j/T = constant. The symbol p_i B(A) refers to the probabilities obtained for Configuration B, using the parameters obtained from fitting Configuration A to the absorption isotherms; p_i A(A) and p_i B(B) are similarly defined.

occurrence of stationary states, it is seen that the LRO model satisfactorily describes the experimental data up to a certain nitrogen content or, equivalently, up to a certain nitriding potential: $y_N = 0.46$ for 773 K and $y_N \simeq 0.43$ for 823 K.

The position and width of the two-phase region for Configurations A and B can be estimated from the phase diagrams presented in Fig. 8 of Ref. 14. The two-phase region extends from about $y_N = 0.41$ to $y_N = 0.42$ for $W_p/RT = -4.48$ and $W_c = \frac{1}{2}W_p$ and from $y_N = 0.355$ to $y_N = 0.37$ for $W_p/RT = -4.48$ and $W_c = W_p$. Since here $W_c = \frac{2}{3}W_p$ (cf. Table 3a), the present two-phase region will have an intermediate width. The Mössbauer results in Fig. 7 hint at a two-phase region from about 0.38 to about 0.42. The discrepancy between the experimental and predicted width of the two-phase region may be due to neglecting the occurrence of short-range order (SRO) of nitrogen atoms and/or to neglecting a dependence of the vibrational entropy on the nitrogen concentration and the type of order in the present LRO model.†

6. SUMMARY AND CONCLUSIONS

Nitrogen-absorption isotherms for the ε-nitride phase determined at a temperature higher than 723 K do not describe equilibrium between the adjusted composition of the gas mixture and the sample but a stationary state at the ε-phase/gas-mixture interface due to the competition between the dissolution of adsorbed nitrogen atoms into ε-nitride and the association of adsorbed nitrogen atoms to molecular nitrogen followed by its desorption.

Nitrogen-absorption isotherms of ε-Fe_2N_{1-z} can be described adequately by a statistical thermodynamics model accounting for LRO of the nitrogen atoms on a hexagonal lattice constituted by the

†For example, for the Cu–Au system, the two-phase region of the $L1_2$ and $L1_0$ phases is predicted to be considerably wider by using the cluster-variation method [27, 28] (incorporating SRO) than by applying a GBW approximation (only incorporating LRO). The result obtained using the cluster-variation method agrees with the experimental Cu–Au phase diagram [29].

octahedral interstices of the h.c.p. iron sublattice. The model adopts the Gorsky–Bragg–Williams approximation and incorporates nearest neighbour interactions in the basal plane of the hexagonal unit cell and in the direction perpendicular to the basal plane, each characterized by an exchange energy: W_p and W_c, respectively. Two ordered configurations of the nitrogen atoms are predicted, denoted as Configuration A and Configuration B. The values for the exchange energies obtained were proportional to the reciprocal of the cube of the distance between neighbouring sites on the interstitial sublattice in the direction pertaining to the exchange energy considered. This indicates that LRO is primarily due to strain-induced interaction caused by misfitting of the nitrogen atoms in the octahedral interstices. The thermodynamics of ε-Fe_2N_{1-z} are described by the LRO model with the exchange energies:

$$\frac{W_p}{RT} = -4.48 \quad \frac{W_c}{RT} = -2.98 \qquad \text{(for } 673 \text{ K} \leq T \leq 723 \text{ K)}$$

and the reference state:

$$\ln r_N^0 = \frac{3.59 \times 10^3}{T} - 4.92$$

with r_N^0 in $Pa^{-1/2}$ and T in K.

X-ray and neutron diffraction analyses confirmed the occurrence of LRO of nitrogen atoms in ε-Fe_2N_{1-z} specimens with various compositions. In general diffraction analysis did not allow distinguishing between the occurrence of ordering according to Configuration A and/or Configuration B. The lattice parameters of the hexagonal unit cell of ε-Fe_2N_{1-z}, used to describe ordering of the nitrogen atoms in the LRO model, were evaluated as a function of the occupied fraction of the hexagonal sublattice of octahedral sites, y_N, for the range $0.33 < y_N < 0.47$ (y_N = at.N/at.Fe):

$$a = 0.44709 + 0.0673\, y_N \text{ (nm)}$$

$$c = 0.42723 + 0.0318\, y_N \text{ (nm)}$$

where $a' = a/\sqrt{3}$ and $c' = c$, a' and c' being the lattice parameters of the h.c.p. sublattice of iron atoms.

Mössbauer spectroscopy allowed four different magnetic environments of the iron atoms in ε-Fe_2N_{1-z} to be distinguished. These environments were attributed to iron atoms surrounded by 1–3 nitrogen atoms. The relative abundances of the various iron environments are consistent with probabilities for these environments calculated from the LRO model for Configuration B at $y_N = 0.33$ and for Configuration A for $y_N > 0.45$. For intermediate values of y_N, the Mössbauer results indicate a two-phase region of Configuration A and Configuration B.

Acknowledgements—We are indebted to Dr R. Helmholdt of ECN in Petten (The Netherlands) for neutron diffraction experiments. Dr ir Th.H. de Keijser is thanked for providing X-ray facilities. The reference ε-$Fe_2N_{2/3}$ powder was kindly supplied by Dipl.-Chem. D. Rechenbach and Professor Dr H. Jacobs of Dortmund University (Dortmund, Germany). Financial support from the Foundation for Fundamental Research of Matter (FOM), the Netherlands Technology Foundation (STW) and IOP-Metalen is gratefully acknowledged.

REFERENCES

1. Jack, K. H., *Proc. R. Soc. Lond.*, 1948, **A195,** 34–55.
2. Jack, K. H., *Acta crystall.*, 1952, **5,** 404–411.
3. Hillert, M. and Staffanson, L.-I., *Acta Chem. Scand.*, 1970, **24**(10), 3618–3626.
4. Harvig, H., *Acta Chem. Scand.*, 1971, **25**(9), 3199–3204.
5. Hillert, M. and Jarl, M., *Metall. Trans. A*, 1975, **6A,** 553–559.
6. Ågren, J., *Metall. Trans. A*, 1979, **10A,** 1847–1852.
7. Kunze, J., *Steel Res.*, 1986, **57,** 361–367.
8. Maldzinski, L., Przylecki, Z. and Kunze, J., *Steel Res.*, 1986, **57,** 645–649.
9. Kunze, J., *Nitrogen and Carbon in Iron and Steels; Thermodynamics*, Physical Research, Vol. 16. Akademie Verlag, Berlin, 1990.
10. Frisk, K., *Calphad*, 1991, **15**(1), 79–106.
11. Du, H., *J. Phase Equilibria*, 1993, **14,** 682–693.
12. Guillermet, A. F. and Du, H., *Z. Metallkd.*, 1994, **85**(3), 154–163.
13. Kooi, B. J., Somers, M. A. J. and Mittemeijer, E. J., *Metall. Mater. Trans. A*, 1996, **27A,** 1055–1061 and 1063–1071.
14. Kooi, B. J., Somers, M. A. J. and Mittemeijer, E. J., *Metall. Mater. Trans. A*, 1994, **25A,** 2797–2814.
15. Gorsky, W. S., *Z. Phys.*, 1928, **50,** 64.
16. Bragg, W. L. and Williams, E. J., *Proc. R. Soc. London*, 1934, **A145,** 699; *Proc. R. Soc. London*, 1935, **A151,** 540; *Proc. R. Soc. London*, 1935, **A152,** 231.
17. Kooi, B. J., Iron–nitrogen phases: thermodynamics, long-range order and oxidation behaviour. Ph.D. thesis, Delft University of Technology, 1995.
18. Somers, M. A. J., Colijn, P. F., Sloof, W. G. and Mittemeijer, E. J., *Z. Metallkd.*, 1990, **81,** 33–43.
19. Wriedt, H. A., Gokcen, N. A. and Nafziger, R. H., *Bulletin of Alloy Phase Diagrams*, 1987, **8**(4), 355–377.
20. Burdese, A., *Metall. Ital.*, 1957, **49,** 195–199.
21. Bouchard, R. J., Frederick, C. G. and Johnson, V., *J. appl. Phys.*, 1974, **45,** 4067–4070.
22. Rechenbach, D., Diplomarbeit Universität Dortmund, Dortmund, 1993.
23. Firrao, D., DeBenedetti, B. and Rosso, M., *Metall. Ital.*, 1979, **71,** 373–381.
24. Hillert, M. and Jarl, M., *Acta metall.*, 1977, **25,** 1–9.
25. Eshelby, J. D., *Acta metall.*, 1955, **3,** 487–490.
26. Khachaturyan, A. G., *Theory of Structural Transformations in Solids*. John Wiley & Sons, New York, 1983.
27. Kikuchi, R. and de Fontaine, D., National Bureau of Standards Special Publication 496, Gaithersburg, 1977, pp. 967–998.
28. de Fontaine, D. and Wolverton, C., *Ber. Bunsengesell. Phys. Chem.*, 1992, **96,** 1503–1512.
29. de Fontaine, D. and Kikuchi, R., National Bureau of Standards Special Publication 496, Gaithersburg, 1977, pp. 999–1026.
30. Grabke, H.-J., *Ber. Bunsengesell. Phys. Chem.*, 1968, **72,** 533–540.
31. Grabke, H.-J., *Ber. Bunsengesell. Phys. Chem.*, 1968, **72,** 541–548.

32. Grabke, H.-J., *Ber. Bunsengesell. Phys. Chem.*, 1969, **73**, 596–601.
33. Somers, M. A. J. and Mittemeijer, E. J., *Surf. Eng.*, 1987, **3**, 123–137.
34. Mittemeijer, E. J., van Rooijen, M., Wierzyllowski, I., Rozendaal, H. C. F. and Colijn, P. F., *Z. Metallkd.*, 1983, **74**, 473–482.
35. Somers, M. A. J. and Mittemeijer, E. J., *Metall. Trans. A*, 1990, **21A**, 189–204.

APPENDIX

Preparation and Stability of Fe–N Phases

At temperatures above about 673 K and at normal pressure ($\sim$1 atm), NH_3 and Fe–N phases tend to decompose into N_2 and H_2 and into N_2 and Fe with a low nitrogen content, respectively. These instabilities pose problems with respect to the definition of the thermodynamic equilibrium of the solid Fe–N phases with the gas phase (see Refs 30–32). Here the preparation of ε-nitride is discussed.

Instability of ammonia

Ammonia gas used for the preparation of the nitrides is thermodynamically unstable at temperatures above about 500 K with respect to decomposition into N_2 and H_2 according to equation (6a). Fortunately, the thermal decomposition of ammonia proceeds slowly in the gas phase. This allows tuning of a specific chemical potential of nitrogen by adjusting the nitriding potential of the flowing gas mixture through the NH_3:H_2 ratio.

At the surface of an ε-nitride sample the decomposition of ammonia can be represented as

$$NH_3 \rightleftarrows N_{ads} + \tfrac{3}{2}H_2 \qquad \text{(A1)}$$

where N_{ads} denotes nitrogen atoms adsorbed at the specimen surface. The adsorbed nitrogen atoms can dissolve into the solid sample (and then are denoted as N_ε):

$$N_{ads} \rightleftarrows N_\varepsilon \qquad \text{(A2)}$$

or they can recombine at the surface to molecular nitrogen and desorb:

$$N_{ads} + N_{ads} \rightleftarrows N_2. \qquad \text{(A3)}$$

If only dissolution of nitrogen into the sample according to equation (A2) occurs, realization of equilibrium according to the sum of equations (A1) and (A2) implies that the chemical potential of nitrogen throughout the sample is equal to the adjusted chemical potential of nitrogen in the gas phase. If, per unit of time, the amount of adsorbed nitrogen atoms combining with molecular nitrogen and additionally desorbing from the surface [equation (A3)] cannot be neglected with respect to the amount of adsorbed nitrogen that dissolves into the sample [equation (A2)], the chemical potential of the nitrogen of the initial, adjusted composition of the ammonia/hydrogen mixture is larger than the chemical potential of nitrogen dissolved in the sample. Then, a stationary state can develop at the sample surface, corresponding to an unknown chemical potential of nitrogen. The tendency for association of the adsorbed nitrogen atoms becomes stronger with increasing number of adsorbed nitrogen atoms and with increasing temperature. Hence, equilibrium studies over the entire composition range of the ε-nitride phase in NH_3/H_2 gas mixtures can be carried out only at a relatively low temperature (e.g. for α-Fe[N] it was observed that the maximum temperature where equilibrium could be attained with the gas mixture was about 773 K [30]; see discussion in Sections 4.1 and 5.3).

Instability of Fe–N phases

The formation of ε-iron nitrides at the surface of an initially pure iron sample proceeds readily in NH_3/H_2 mixtures, provided the chemical potential of nitrogen imposed at the sample surface allows its formation. In the interior of the sample, where this chemical potential (apparent nitrogen partial pressure) is not imposed, a large driving force exists for N_2 development of the dissolved nitrogen atoms, especially at temperatures above about 750 K and for relatively high nitrogen contents. The precipitation of N_2-gas leads to cavities in the sample during nitriding. Such cavities can grow and coalesce, leading to the establishment of pores (channels) that connect the interior of the sample with the outer gas mixture [33]. This mechanism of decomposition has been observed to occur for all Fe–N phases [33 35].

In a very porous iron foil, the large surface area with the gas mixture and the short distances to be bridged by solid-state diffusion promote the fast establishment of equilibrium or a stationary state.